A discrete method to study stochastic growth equations: a cellular automata perspective

2007 J. Phys. A: Math. Theor. 40 13245

(http://iopscience.iop.org/1751-8121/40/44/006)

IOP PUBLISHING JOURNAL OF PHYSICS A: MATHEMATICAL AND THEORETICAL

J. Phys. A: Math. Theor. **40** (2007) 13245–13256 doi:10.1088/1751-8113/40/44/006

A discrete method to study stochastic growth equations: a cellular automata perspective

T G Mattos[1,3], J G Moreira[1] and A P F Atman[2]

[1] Departamento de Física, Instituto de Ciências Exatas, Universidade Federal de Minas Gerais, CP 702, CEP 30161-123, Belo Horizonte MG, Brazil
[2] Centro Federal de Educação Tecnológica (CEFET-MG), CEP 30510-000 Belo Horizonte MG, Brazil

E-mail: tgmattos@if.uff.br

Received 12 July 2007, in final form 25 September 2007
Published 16 October 2007
Online at stacks.iop.org/JPhysA/40/13245

Abstract

Using cellular automata dynamics, a discrete technique to study stochastic growth equations (SGE) is presented. By analogy to deposition models in which the growth rule depends on height differences between neighbours, we introduce an interface growth process with synchronous updating in which the transition probability for a given site i to receive a particle at a time t is defined as $p_i(t) = \rho \exp[\kappa \Gamma_i(t)]$. ρ and κ are the model parameters and $\Gamma_i(t)$ is a function which depends on the height of the site i and its neighbours, and its functional form is specified through discretization of the deterministic part of the growth equation associated with a given deposition process. To validate the method, we study its application to two linear SGE—the Edwards–Wilkinson equation and the Mullins–Herring equation, and a nonlinear one—the Kardar–Parisi–Zhang equation. The statistical analysis of the height distributions in simulations recovered the correct values for roughening exponents, confirming that the processes generated are indeed in the universality classes of the original growth equations. We also observed a crossover from random deposition to the correlated regime when the parameter κ is varied in each case studied.

PACS numbers: 89.75.Da, 02.50.−r, 68.35.Ct, 05.10.−a

1. Introduction

In order to better understand several features observed in a wide range of physical processes, discrete computational growth models have been largely employed in the last few decades to investigate interface growth phenomena [1–3]. An emblematic feature common to several models is the kinetic roughening of the height profiles, as observed in the Eden model [4],

[3] Present address: Instituto de Física, Universidade Federal Fluminense, Avenida Litorânea s/n, CEP 24210-340 Niterói RJ, Brazil.

the ballistic deposition model [5] and other solid-on-solid growth models in which correlation mechanisms are present. These mechanisms, such as surface relaxation [6], height difference restriction [7], curvature restriction [8] and surface diffusion [9, 10] are associated with different universality classes (UCs). These UCs are also associated with experimental studies of growing interfaces (e.g., generated by molecular beam epitaxy or vapour deposition on cold substrates—see [2, 3] and references therein), and with theoretical descriptions based on stochastic growth equations.

The theoretical framework developed to study interface growth phenomena has also been applied to investigate cellular automata (CA)—a huge class of computational models which can describe many phenomena in a wide range of scientific fields [11]. By means of an accumulation method [12], it is possible to map the spatiotemporal evolution of a CA into growing interfaces, and then apply the usual methodology to analyse these systems. Recently, this method has been used to study deterministic [13] and probabilistic CA [14, 15].

The major tool commonly used to study the interface growth is the quantitative analysis of the temporal evolution of the height profile roughness (or width) $\omega(L, t)$, which is defined as

$$\omega^2(L, t) = \frac{1}{L}\sum_{i=1}^{L}[h_i(t) - \overline{h}(L, t)]^2, \tag{1}$$

where L is the size of the substrate and $\overline{h}(L, t)$ is the mean height of the generated profile.

For discrete deposition models in finite substrates it is known that, for short times, the width grows as a power law of t, defining the growth exponent β. After the saturation time t_x, the interface reaches a stationary regime and the roughness saturates. Both the saturation roughness ω_{sat} and the saturation time t_x depend on the system size L, as power laws, defining the roughness exponent α and the dynamic exponent z, respectively. The surface roughness obeys the Family–Vicsek scaling law [16]

$$\omega(L, t) \sim L^{\alpha} f\left(\frac{t}{L^z}\right), \tag{2}$$

where the scaling function $f(u)$ behaves as $f(u) \sim u^{\beta}$ for $u \ll 1$, and $f(u) =$ constant for $u \gg 1$. It follows that $\beta = \alpha/z$.

For a given dimension, a set of values for the roughening exponents characterizes an UC. Thus, if two or more processes have the same values for the roughening exponents, one can say that they belong to the same UC; it implies that they share the same underlying dynamics, symmetries and conservation laws.

Based on certain symmetries, it is possible to construct stochastic growth equations (SGE) associated with different UCs [2]. This continuum approach often provides analytical results for the roughening exponents in the respective UC and, sometimes, exact values can be obtained for all dimensions.

In this paper, we consider two linear equations and one nonlinear one. They are, respectively, the Edwards–Wilkinson (EW) equation [17],

$$\frac{\partial h(\mathbf{x}, t)}{\partial t} = \nu\nabla^2 h(\mathbf{x}, t) + \eta(\mathbf{x}, t), \tag{3}$$

that can be associated with the random deposition with the surface relaxation model [6]; and the Mullins–Herring (MH) equation [18, 19],

$$\frac{\partial h(\mathbf{x}, t)}{\partial t} = -K\nabla^4 h(\mathbf{x}, t) + \eta(\mathbf{x}, t), \tag{4}$$

which is associated with deposition models with surface diffusion [9, 10].

In the nonlinear case, the Kardar–Parisi–Zhang (KPZ) equation [20],

$$\frac{\partial h(\mathbf{x}, t)}{\partial t} = \nu \nabla^2 h(\mathbf{x}, t) + \frac{\lambda}{2} (\nabla h)^2 + \eta(\mathbf{x}, t), \tag{5}$$

has attracted most of the attention in the literature. This equation can be associated with two discrete models: the ballistic deposition [5] and the restricted solid-on-solid growth model [7].

In these equations, $h(\mathbf{x}, t)$ is the local height profile, assumed to be continuous (eventual hangovers are ignored), and $\eta(\mathbf{x}, t)$ is a Gaussian noise, with zero mean and correlation given by

$$\langle \eta(\mathbf{x}, t) \eta(\mathbf{x}', t') \rangle = 2D\delta^d(\mathbf{x} - \mathbf{x}')\delta(t - t'). \tag{6}$$

Analytical results for the linear SGE furnish exact values for the roughening exponents. For the EW equation (3), the exponents for a d-dimensional substrate are [17, 21]

$$\alpha = \frac{2-d}{2}, \qquad \beta = \frac{2-d}{4} \qquad \text{and} \qquad z = 2, \tag{7}$$

while the solution for the MH equation (4) yields [9, 10]

$$\alpha = \frac{4-d}{2}, \qquad \beta = \frac{4-d}{8} \qquad \text{and} \qquad z = 4. \tag{8}$$

There is no general analytical solution for the KPZ equation (5). However, for $d = 1$, the renormalization group theory prescribes [20]

$$\alpha = \tfrac{1}{2}, \qquad \beta = \tfrac{1}{3} \qquad \text{and} \qquad z = \tfrac{2}{3}. \tag{9}$$

Crossovers between distinct UCs are a topic of great interest as well. Particular attention has been devoted to the study of competitive growth models where two different types of particles are deposited, one with probability P and the other one with probability $(1 - P)$, yielding to several combinations of crossovers between different growth processes [22, 23]. Specifically, models mixing correlated growth dynamics with random deposition (RD) dynamics have been investigated by means of simulations and scaling arguments [24, 25]. A crossover from the KPZ to EW class has also been observed in large scale simulations of a deposition model with restricted surface relaxation [26].

Our principal aim in this paper is to introduce a discrete method based on CA dynamics to study stochastic growth equations (SGE). This method has already been applied to study the EW equation [27] and, in this paper, we extend it to other models, present more accurate results and develop its basic theoretical concepts. Using a simple discretization scheme, it is possible to obtain numerical solutions for the roughening exponents without actually having to solve the associated growth equation. This means that the method can be applied to equations whose solutions are not known. In section 2 we outline the main features of the method, such as the definitions of the parameters (as well as their range of interest), discretization schemes and a brief description of the CA algorithm. In section 3, the numerical results for the roughening exponents corresponding to each UC considered are shown. In section 4, a brief description of the crossover from RD to correlated growth as a function of a parameter is presented. Finally, in section 5, we draw some conclusions and perspectives.

2. The method

The time evolution for the height profile of a growing interface could be expressed as a general SGE

$$\frac{\partial h(\mathbf{x}, t)}{\partial t} = B\left(h(\mathbf{x}, t)\right) + C\left(h(\mathbf{x}, t)\right) \eta(\mathbf{x}, t), \tag{10}$$

where $\eta(\mathbf{x}, t)$ is a white noise and $B\,(h(\mathbf{x}, t))$ and $C\,(h(\mathbf{x}, t))$ are specified in each case. For example, with $B = 0$ and $C = 1$, we can write

$$\frac{\partial \mathcal{W}(\mathbf{x}, t)}{\partial t} = \eta(\mathbf{x}, t), \tag{11}$$

where $\mathcal{W}(\mathbf{x}, t)$ describes a Brownian motion.

Choosing $C = 1$, $B = \mathcal{D}h(\mathbf{x}, t)$ and after some manipulation, we can write

$$\mathrm{d}h(\mathbf{x}, t) = \mathcal{D}h(\mathbf{x}, t)\mathrm{d}t + \mathrm{d}\mathcal{W}(\mathbf{x}, t), \tag{12}$$

where $\mathcal{D}$ is a general operator. This general form for an SGE could describe (3), (4) or (5). With the integration factor $\mathrm{e}^{-t\mathcal{D}}$, (12) can be rewritten as

$$\mathrm{e}^{-t\mathcal{D}}\mathrm{d}h(\mathbf{x}, t) - \mathrm{e}^{-t\mathcal{D}}\mathcal{D}h(\mathbf{x}, t)\,\mathrm{d}t = \mathrm{e}^{-t\mathcal{D}}\mathrm{d}\mathcal{W}(\mathbf{x}, t). \tag{13}$$

Using the Ito formulæ [28], which coincides with the ordinary calculus in this case, we have

$$\mathrm{d}(\mathrm{e}^{-t\mathcal{D}}h(\mathbf{x}, t)) = \mathrm{e}^{-t\mathcal{D}}\,\mathrm{d}\mathcal{W}(\mathbf{x}, t). \tag{14}$$

Integration of the last equation yields

$$h(\mathbf{x}, t) = \mathrm{e}^{t\mathcal{D}}h(\mathbf{x}, 0) + \int_0^t \mathrm{e}^{(t-\tau)\mathcal{D}}\,\mathrm{d}\mathcal{W}(\mathbf{x}, \tau), \tag{15}$$

which is the general solution for $h(\mathbf{x}, t)$. The second term on the right-hand side describes the fluctuations in the deposition process and the first term represents a time evolution operator, $\mathrm{e}^{t\mathcal{D}}$, acting on the initial state $h(\mathbf{x}, 0)$. This form for the time evolution operator is the major motivation for the expression of the CA transition probability presented below.

In our simulations, we consider a one-dimensional lattice with linear extension L, initially flat, with periodic boundary conditions and synchronous updating. Site i receives a particle at time t with the probability $p_i(t)$ given by

$$p_i(t) = \rho \exp\left[\kappa\Gamma_i(t)\right]. \tag{16}$$

Here, $0 < \rho < 1$ and $\kappa > 0$ are two parameters, kept fixed throughout the evolution of the interface. The former is related to the profile growth speed and the later can be associated with an inverse of temperature, considering an analogy with vapour deposition: the synchronous update scheme can be thought as attempts for deposition of vapour particles on a cold substrate, allowing the development of growing structures. $\Gamma_i(t)$ is the kernel, a function which depends on heights of site i and its neighbourhood, at time t. Its explicit form is given by the discretization of the deterministic part of the growth equation intended to study and it simulates the operator $\mathcal{D}$.

In the case of (3), the kernel is given by the discretization of the Laplacian $\nabla^2 h$,

$$\Gamma_i(t) = h_{i+1}(t) + h_{i-1}(t) - 2h_i(t). \tag{17}$$

For (4), the kernel follows from the discretization of the negative of the fourth spatial derivative, $-\nabla^4 h$,

$$\Gamma_i(t) = -\left[6h_i(t) + h_{i+2}(t) + h_{i-2}(t)\right] + 4\left[h_{i+1}(t) + h_{i-1}(t)\right]. \tag{18}$$

Finally, the discretization of the square of the gradient, $(\nabla h)^2$, and of the Laplacian, yield the kernel for (5),

$$\Gamma_i(t) = \frac{1}{\varepsilon}\left[h_{i+1}(t) - h_{i-1}(t)\right]^2 + \left[h_{i+1}(t) + h_{i-1}(t) - 2h_i(t)\right], \tag{19}$$

where $\varepsilon > 0$ is the parameter which controls the nonlinearity strength: large ε yields small contribution of the nonlinear term relative to the linear one, and conversely.

So far we have explicitly considered only the deterministic part of the growth differential equations, (3) to (5); the stochastic nature of these equations, expressed by the white noise $\eta(\mathbf{x}, t)$, is simulated in our method implicitly, through the probabilistic character of the growth process. We have done rigorous studies of the symmetry and decay properties of the height profile distributions, which are all in accordance with the predicted behaviour for Gaussian distributions, exactly which is expected when white noise is present.

It is important to note that eventually it is possible to obtain $p_i(t) > 1$. To overcome this situation, we impose the condition

$$p_i(t) \geqslant 1 \Longrightarrow p_i(t) = 1 \Longrightarrow h_i(t+1) = h_i(t) + 1. \tag{20}$$

Hence, for a given pair (ρ, κ), there is a maximum kernel value, $\Gamma_{\max}(\rho, \kappa)$, such that

$$\Gamma_i(t) \geqslant \Gamma_{\max} \Longrightarrow p_i(t) = 1. \tag{21}$$

Making $p_i(t) = 1$ in (16) and having in mind the fact that $\Gamma_i(t)$ is an integer by definition, we find

$$\Gamma_{\max}(\rho, \kappa) = \operatorname{int}\left(-\frac{1}{\kappa}\ln\rho\right). \tag{22}$$

Moreover, the minimal value for $\Gamma_{\max}$ should be one; otherwise, if $\Gamma_{\max} = 0$, the algorithm would make the interface grow flat since the beginning of the process, and no scaling features would be observed. This condition imposes a restriction for the range of allowed values of the parameter κ,

$$\Gamma_{\max} \geqslant 1 \Longrightarrow \kappa \leqslant \ln\left(\frac{1}{\rho}\right). \tag{23}$$

In the simulations, we fixed $\rho = \frac{1}{2}$ which means that starting from a flat surface, initially each site has a probability $p = \frac{1}{2}$ to receive a particle. A further analysis of the displacement rate of the mean height showed that the parameter ρ is related to the profile growth speed.

Basically, for each time step t, the algorithm does the following: (i) calculate $\Gamma_i(t)$; (ii) ask whether $\Gamma_i(t) \geqslant \Gamma_{\max}$; (iii) if so, a particle should be deposited in site i; if not, a random number r is taken in the range [0, 1) and $p_i(t)$ is calculated: if $r < p_i(t)$, a particle should be deposited on site i; (iv) repeat steps (i)–(iii) for $i = 1, \ldots, L$; (v) those sites which received a particle have their heights increased by unit (synchronous updating scheme).

It should be mentioned that the choice of the exponential form in (16) is possibly not unique. Nevertheless we chose it due to the form of the time evolution operator in (15), which is the formal solution to the general problem of a SGE, as stated in (10).

3. Roughening exponents

In this section, we show the results obtained for the roughening exponents for each one of the three UCs studied. Typically, with a lattice of size $L = 10^4$, we initially fixed $\kappa = 10^{-1}$ and averaged the results over 50 independent samples.

In figure 1, we show the results for the interface roughness of the profiles generated by the application of the method in the EW and MH equations. Note the good agreement between the growth exponent values obtained in our simulations to those predicted by (7) and (8), in $d = 1$.

In the nonlinear case, our simulations have shown different situations: when the contribution from the Laplacian vanishes ($\varepsilon \to 0$) and the system evolves following a pure nonlinear dynamics, one obtains persistent unevennesses growing between 'valleys' and 'hills', since the square of the gradient induces equally the development of such structures. We can

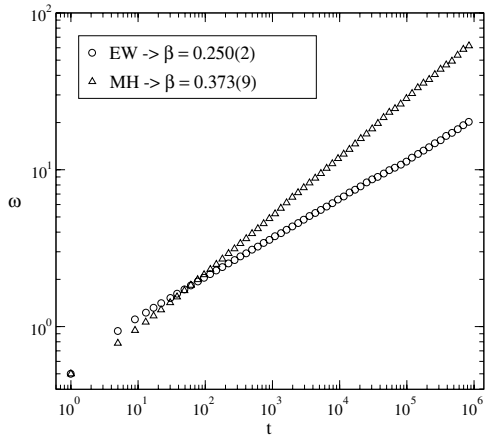

Figure 1. Log–log plots of the roughness as a function of time, for $\rho = 1/2$, $\kappa = 10^{-1}$, $L = 10^4$ and averaged over 50 independent samples. The circles represent the data for the EW class ($\beta = 1/4$ expected), while the triangles are the data for the MH class ($\beta = 3/8$ expected). The least-squares method was used in order to determine the indicated numerical values for β.

see in the top frame of figure 2 the evolution of a profile generated in the pure nonlinear case, where the set of probabilities reaches a stable configuration such that p_i = constant for all i: sites with larger heights have $p_i = 1$ and sites in the valleys have $p_i = \rho$ (these valleys are symmetric, i.e. both sides have same slope). At this stage, the interface roughness (which is a measure of the interface width and can be estimated by the height difference between the maximum and the minimum of the profile) grows linearly with time; thus, it implies that $\beta = 1$. This behaviour is shown in the bottom of figure 2. It is worthy to mention that this behaviour is independent of the size of the system and occurs for all tested values of κ. A crossover from $\beta = 1/2$ to $\beta = 1$ is observed, and the crossover time increases when κ decreases.

In the top of figure 3, we show the profiles generated for intermediary values of ε ($\varepsilon = 2$), which correspond to a small, but non-vanishing, contribution from the Laplacian term. In this case the method produces crystallized patterns with asymmetric hills and valleys, in which all sites i have $p_i(t) = 1$ for all t (after a certain transient time) and the roughness no longer changes. In the bottom of figure 3 we show the behaviour of the roughness for several system sizes and, as one can see, for larger systems the roughness grows initially with $\beta \approx 1/3$ before the frozen configuration is reached, while smaller systems can saturate before that. We believe that these structures are attractors among the possible configurations of heights in the profile. So, for small ε, the system always reaches such absorbing configurations. In our simulations, the size of the system was restricted to $L \leqslant 10^5$; thus, we chose $\varepsilon > 4$ in order to obtain the standard behaviour of the roughness and avoid such anomalous configurations.

We show in figure 4(a) the results obtained for the temporal evolution of the profile roughness when $\varepsilon = 5$. Again, good agreement with the prediction was obtained for the growth exponent β. For larger values of ε, a crossover from $\beta = 1/4$ to $\beta = 1/3$ regimes is observed, as shown in figure 4(b), where $\varepsilon = 10$ and $L = 10^5$. The explanation for this crossover is the following: at the beginning of the growth process, when the roughness is not large enough, the quadratic term of the KPZ equation is much smaller than the Laplacian term; so, the linear regime dominates and $\beta \approx 1/4$. As the roughness increases, the nonlinear

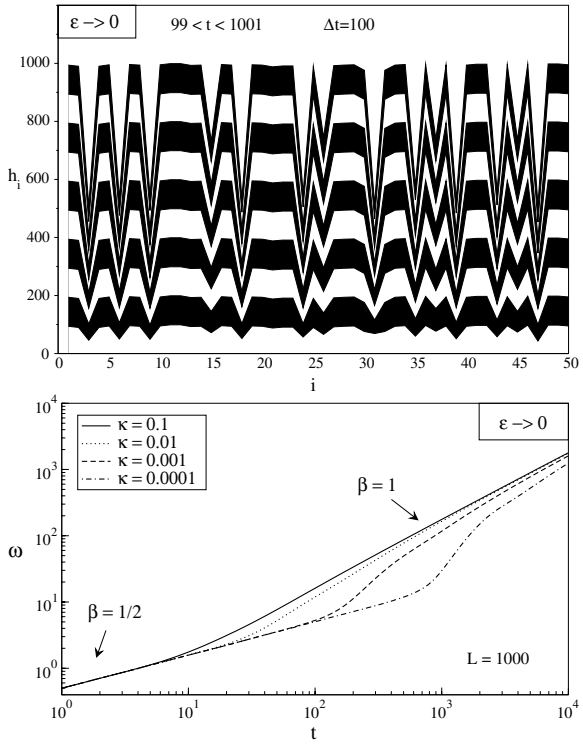

Figure 2. In the top frame we show the evolution of the profiles by changing the colour of the particles each 10^2 time steps, for $10^2 \leqslant t \leqslant 10^3$, in the limiting case of $\varepsilon \to 0$. In the bottom we display the log–log plot of the time behaviour of the roughness for $L = 10^3$ and several values of κ between 10^{-1} and 10^{-4}. Note that for smaller values of κ the crossover $\beta = 1/2 \to \beta = 1$ occurs at larger times.

term becomes dominant and we get $\beta \approx 1/3$. Of course, if $\varepsilon \to \infty$, this crossover no longer occurs and the results expected for the EW class are recovered. Another crossover between these UCs has been previously obtained by da Silva and Moreira [26] in a deposition model with restricted surface relaxation, where particles can relax only within a given distance s. If a minimum cannot be found in this range, the particle evaporates in a way similar to the restricted solid-on-solid growth model [7]. An s-dependent crossover from $\beta = 1/4$ to $\beta = 1/3$ was obtained by the authors.

To determine the roughness exponent α and the dynamic exponent z, in order to have a complete characterization of each UC, we varied the size L of the lattice, but still holding $\kappa = 0.1$ fixed. We made $L = 25, 50, 100, 200, 300$ and 400 for the EW and KPZ equations. In the MH class, for which $z = 4$, we had to restrict our simulations to $L = 20, 25, 30, 40, 50$ and 60, due to the impracticable saturation times for larger systems. The results are presented in figure 5: in the left column, we show the roughness temporal behaviour for several values of L; in the right column, we apply the Family–Vicsek scaling law (2) using the corresponding values for α and z expected in each UC, leading to the collapse of the various curves into a single one. The remarkable collapses obtained, corroborated by the obtained values for β, are sufficient to guarantee that our method reproduces correctly each one of the three UCs.

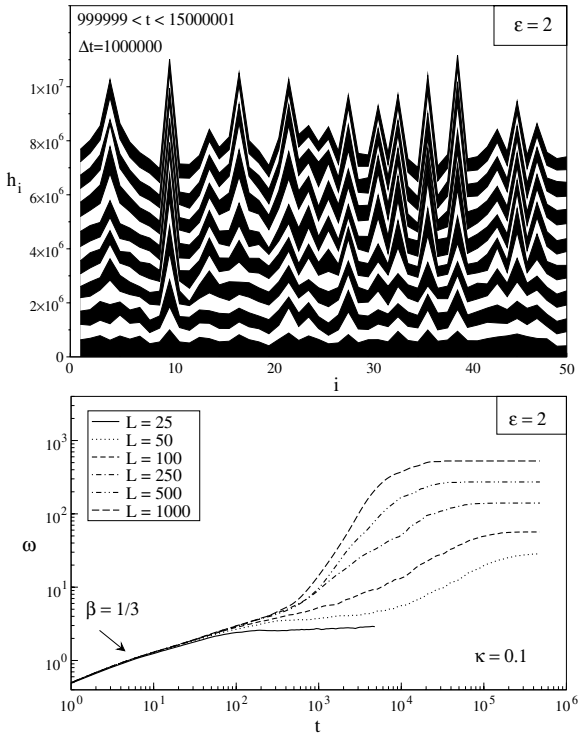

Figure 3. In the top frame we show the interface evolution for the case of $\varepsilon = 2$, for $10^6 \leqslant t \leqslant 1.5 \times 10^7$, where we change the colour of the particles each 10^6 steps. In this case the system is very close to a crystallized pattern. In the bottom we have $\kappa = 10^{-1}$ and several values of L in the range $25 \leqslant L \leqslant 10^3$: larger systems reach crystallized patterns while smaller ones can saturate before that happens.

4. Crossover from random to correlated growth

We identify a crossover from the RD regime ($\beta = 1/2$) to the corresponding correlated process when we vary the parameter κ and this crossover does not depend on the system size L.

Defining the crossover time as t_c, we observed that t_c, the saturation roughness ω_{sat} and the saturation time t_x are all power-law functions of the parameter κ,

$$t_c \sim \kappa^{-z'_\kappa}, \qquad t_x \sim \kappa^{-z_\kappa}, \qquad \omega_{sat} \sim \kappa^{-\alpha_\kappa}. \tag{24}$$

The left graph in figure 6 shows the behaviour of the roughness for different values of κ, considering the EW equation: we consider $L = 250$, $\kappa = 10^{-1}, 10^{-2}$ and 10^{-3}, and average over 40 independent samples. The right graph in figure 6 shows the log–log plot $t_c \times \kappa$. Using a power-law fitting we have obtained $z'_\kappa = 1.02(2)$. In figure 7, we show the curves of saturation time and saturation roughness against κ. As shown, we found $z_\kappa = 1.04(3)$ and $\alpha_\kappa = 0.509(2)$.

For the other two classes, MH and KPZ, we have found values for the κ-exponents very close to those obtained for the EW class. Thus, we conclude that the crossover from the random to correlated regime does not depend on the mechanism that generates correlations in the system. It is worthy to mention that for the KPZ class, when this crossover from random

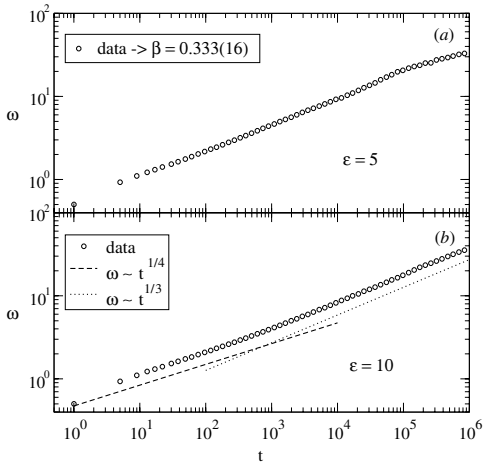

Figure 4. Log–log plots of the roughness as a function of time, in the application to the KPZ equation, where $\beta = 1/3$ is expected. In the top, we have $\varepsilon = 5$ for a system of size $L = 10^4$. In the bottom, $\varepsilon = 10$ and $L = 10^5$, where a crossover from $\beta = 1/4$ to $\beta = 1/3$ is observed. We have drawn the functions $\omega \sim t^{1/4}$ (dashed line) and $\omega \sim t^{1/3}$ (dotted line) for comparison.

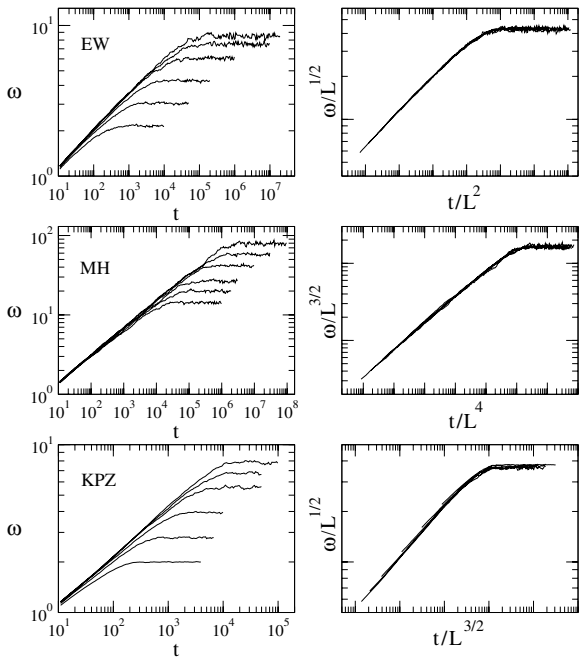

Figure 5. Log–log plots of the roughness for various system sizes L, in the three applications of the method (left column). As we apply the Family–Vicsek scaling law, using the expected exponents for each UC, good collapses are obtained (right column).

to correlated growth occurs, the Laplacian term dominates and the crossover should always be from random to linear correlated growth.

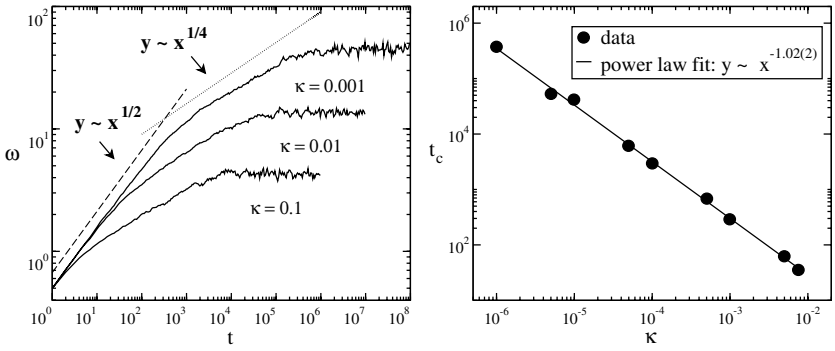

Figure 6. In the left panel, the temporal behaviour of the roughness for $L = 250$ and $\kappa = 10^{-1}, 10^{-2}$ and 10^{-3}, averaged over 40 samples, in the application to the EW class. The crossover between $\beta = 1/2$ (RD) and $\beta = 1/4$ (EW) can be seen by comparing the curves with the dashed and dotted lines. In the right, the crossover time t_c plotted against κ exhibiting a power law with exponent $z'_\kappa = 1.02(2)$.

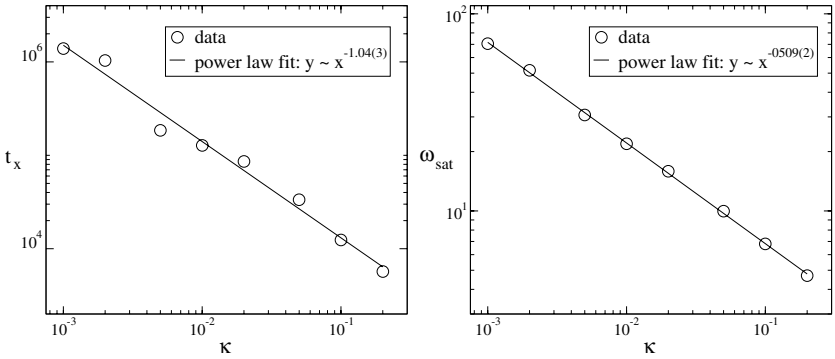

Figure 7. Saturation time (left) and saturation roughness (right) as functions of the parameter κ, for a system of size $L = 250$ and averaged over 40 samples. From the power-law fits we have obtained $z_\kappa = 1.04(3)$ and $\alpha_\kappa = 0.509(2)$.

The fact that we have found $z_\kappa \cong z'_\kappa \cong 1$ shows that κ^{-1} plays the role of a characteristic time factor in the evolution of the system. Furthermore, z'_κ and z_κ must have the same value because, otherwise, making κ small enough we would have either the uncorrelated regime taking place over the correlated one (for the case $z'_\kappa > z_\kappa$), or the correlated behaviour stretching over and over (for $z'_\kappa < z_\kappa$), what cannot happen unless that the system size is increased. In other words, the quantity $t_x - t_c$ is supposed to be a function only of the system size L.

Another result obtained, $\alpha_\kappa \cong z'_\kappa/2$, can be understood as follows. When $t = t_c$, the roughness value is, for example, $\omega = \omega_c$; as until this moment the system is under uncorrelated regime ($\beta = 1/2$), we have $\omega_c = t_c^{1/2}$. It is also clear that $\omega_c \sim \omega_{sat}$, thus

$$\omega_c \sim \omega_{sat} \Longrightarrow t_c^{1/2} \sim \omega_{sat} \Longrightarrow \kappa^{z'_\kappa/2} \sim \kappa^{\alpha_\kappa} \Longrightarrow \alpha_\kappa = z'_\kappa/2. \tag{25}$$

5. Conclusions and perspectives

We have introduced a discrete method, based on CA dynamics, to study stochastic differential equations associated with discrete deposition models. The method provides a powerful tool for obtaining the roughening exponents, which depends only on the discretization of the deterministic part of the associated stochastic growth equation, with no need to actually solve it.

We have applied this method to study two linear equations (EW and MH equations) and a nonlinear one (KPZ equation), in $d = 1$. The values obtained for the roughening exponents are in good agreement with predictions, showing that the method indeed reproduces each one of the three UCs considered. In particular, for the nonlinear case studied, a crossover from the EW to KPZ class was obtained, for suitable values of parameter ε, which controls the nonlinearity strength.

In addition, a crossover from the RD to correlated regime is obtained when the parameter κ is varied. The crossover time, saturation time and saturation roughness were found to behave as power laws with κ, with numerical exponents $z'_\kappa = 1.02(2)$, $z_\kappa = 1.04(3)$ and $\alpha_\kappa = 0.509(2)$, respectively. These values have shown to be nearly the same, independently of the considered class.

In further works, we intend to apply this method to growth equations in which other terms appear, such as $\nabla^2(\nabla h)^2$ and $\nabla \cdot (\nabla h)^3$, which are the corrections up to the fourth order to the $\nabla^2 h$ term in the EW equation [30], as well as verify the validity of the method to growth processes in two-dimensional lattices, where discretization schemes are not as trivial as in one dimension.

Acknowledgments

The authors would like to thank Emmanuel A Pereira, Fábio D A Aarão Reis and Daniel Cavalcanti for helpful criticisms on the manuscript. This work was supported by Brazilian agency CNPq.

References

[1] Family F and Vicsek T 1991 *Dynamics of Fractal Surfaces* (Singapore: World Scientific)
[2] Barabási A-L and Stanley H E 1995 *Fractal Concepts in Surface Growth* (Cambridge: Cambridge University Press)
[3] Meakin P 1998 *Fractals, Scaling and Growth Far from Equilibrium* (Cambridge: Cambridge University Press)
[4] Eden M 1961 Biology and problems of health *Proc. 4th Berkeley Symp. on Mathematical Statistics and Probability* vol IV (Berkeley, CA: University of California Press)
[5] Meakin P, Ramanlal P, Sander L M and Ball R C 1986 *Phys. Rev.* A **34** 5091
[6] Family F 1986 *J. Phys. A: Math. Gen.* **19** L441–L446
[7] Kim J M and Kosterlitz J M 1989 *Phys. Rev. Lett.* **62** 2289
[8] Kim J M and Das Sarma S 1993 *Phys. Rev.* E **48** 2599–602
[9] Wolf D E and Villain J 1990 *Europhys. Lett.* **13** 389–94
[10] Das Sarma S and Tamborenea P 1991 *Phys. Rev. Lett.* **66** 325–8
[11] Wolfram S 1986 *Theory and Applications of Cellular Automata* (Singapore: World Scientific)
Wolfram S 1983 *Rev. Mod. Phys.* **55** 601–44
[12] de Sales J A, Martins M L and Moreira J G 1999 *J. Phys. A: Math. Gen.* **32** 885
[13] Mattos T G and Moreira J G 2004 *Braz. J. Phys.* **34** 448–51
[14] Atman A P F and Moreira J G 2000 *Eur. Phys. J.* B **16** 501
[15] Atman A P F, Dickman R and Moreira J G 2002 *Phys. Rev.* E **66** 016113
[16] Family F and Vicsek T 1985 *J. Phys. A: Math. Gen.* **18** L75–81
[17] Edwards S F and Wilkinson D R 1982 *Proc. R. Soc. Lond.* A **381** 17–31

[18] Herring C 1951 *The Physics of Powder Metallurgy* (New York: McGraw-Hill)
[19] Mullins W W 1957 *J. Appl. Phys.* **28** 333
Mullins W W 1959 *J. Appl. Phys.* **30** 77
[20] Kardar M, Parisi G and Zhang Y C 1986 *Phys. Rev. Lett.* **56** 889
[21] Nattermann T and Tang L-H 1992 *Phys. Rev.* A **45** 7156–61
[22] Aarão Reis F D A 2002 *Phys. Rev.* E **66** 027101
Aarão Reis F D A 2003 *Phys. Rev.* E **68** 041602
[23] Muraca D, Braunstein L A and Buceta R C 2004 *Phys. Rev.* E **69** 065103(R)
Braunstein L A and Lam C-H 2005 *Phys. Rev.* E **72** 026128
[24] Kolakowska A, Novotny M A and Verma P S 2004 *Phys. Rev.* E **70** 051602
Kolakowska A, Novotny M A and Verma P S 2006 *Phys. Rev.* E **73** 011603
[25] Aarão Reis F D A 2006 *Phys. Rev.* E **73** 021605
[26] da Silva T J and Moreira J G 2002 *Phys. Rev.* E **66** 061604
[27] Mattos T G, Moreira J G and Atman A P F 2006 *Braz. J. Phys.* **36** 746–9
[28] Øskendal B K 1998 *Stochastic Differential Equations: an Introduction with Applications* (Berlin: Springer)
[29] Chien C-C, Pang N-N and Tzeng W-J 2004 *Phys. Rev.* E **70** 021602
[30] Lai Z-W and das Sarma S 1992 *Phys. Rev. Lett.* **69** 3792